Localized CO_2 laser treatment and post-heating process to reduce the growth coefficient of fused silica surface damage

Shizhen Xu (徐世珍)[1*], Xiaotao Zu (祖小涛)[1], and Xiaodong Yuan (袁晓东)[2]

[1] *School of Physical Electronics, University of Electronic Science and Technology of China, Chengdu 610054, China*

[2] *Research Center of Laser Fusion, China Academy of Engineering Physics, Mianyang 621900, China*

[*] *Corresponding author: cecyxsz@yahoo.com.cn*

Received December 7, 2010; accepted January 6, 2011; posted online April 28, 2011

The lifetime of optical components in high-fluence ultraviolet (UV) laser applications is typically limited by laser-initiated damage and its subsequent growth. Using 10.6-μm CO_2 laser pulses, we successfully mitigate 355-nm laser induced damage sites on fused silica surface with dimensions less than 200 μm. The damage threshold increases and the damage growth mitigates. However, the growth coefficients of new damage on the CO_2 laser processed area are higher than those of the original sample. The damage grows with crack propagation for residual stress after CO_2 laser irradiation. Furthermore, post-heating is beneficial to the release of residual stress and slows down the damage growth.

OCIS codes: 140.3330, 160.6030, 140.3390, 140.3470.

doi: 10.3788/COL201109.061405.

Fused silica has excellent optical, thermal, and mechanical properties, and has been commonly used in the manufacture of optical elements, such as windows, lenses, and diffractive optical elements, particularly for inertial confinement fusion (ICF) class lasers. Laser damage of optical components is a main issue for high power laser systems[1]. Exposure of fused silica to a 351-nm laser in the nanosecond regime causes material modifications of stress, cracks, and absorption[2,3]. Growth of nanosecond laser-initiated damage sites under successive irradiation is essentially a lifetime limiter of components, and it increases the operating costs of large-aperture fusion-class laser systems[4,5]. To avoid damage site growth, one of the most promising methods is the use of a CO_2 laser operating at 10.6 μm to locally melt and evaporate the silica damage surface by producing typically smooth, Gaussian-shaped pits[6−9]. The successful demonstration of this method was used to mitigate not only damage sites of less than ∼100 μm in their transverse dimensions[6,7], but also of large craters through spiral-type raster scanning[8]. Some parametric studies have been conducted in order to determine the optimum irradiation conditions[9−12]. Studies on downstream intensification effects associated with the perturbation to the optical surface profile following the mitigation process were also conducted[13]. Material structural changes, stress generation, and defect population induced by CO_2 laser processing of damage have also been investigated[1,14,15]. However, new damage sometimes occurs and the damage growth of new damage sites on CO_2 laser mitigated zone remains unclear.

In this letter, the 355-nm laser induced damage sites are mitigated using CO_2 laser pulses. Laser damage resistance of the treated sites is also investigated. The damage growth coefficients of the new damage sites on CO_2 laser mitigated zone under 355-nm pulses are also measured. Although debris from redeposited silica is eliminated and the stress area is modified, residual stress still exists after the application of a suitable second laser heating[16] and is still prone to damage. Hence, post-annealing is used to release the residual stresses of CO_2 laser mitigation. The effect of post-heating treatment on the damage growth coefficient of fused silica is studied.

Ultraviolet (UV) grade synthetic amorphous silicon dioxide, Corning 7980, with dimensions of 60×40×5 (mm) and a surface micro-roughness of 0.65 nm, was used. Bare fused silica flat optics for testing was acid-etched using a buffered HF solution (1% HF+15% NH_4F) for 10 min to remove embedded polishing contaminants and subsurface damage[17,18].

The TEM_{00} output beam of an air-cooled CO_2 laser (Coherent, GEM-100L) operating at 10.6 μm was used to mitigate the 355-nm laser-induced damage sites. The laser beam focused by a ZnSe lens had a diameter of 1 mm. The power of CO_2 laser was about 7 W with mild treatment. Power control was achieved through pulsed width modulation at a frequency of 10 kHz: a duty cycle of 4% corresponded to a power of 7 W. The number of CO_2 pulses sent on the samples for mitigation was controlled by the exposure time. The CO_2 laser was exposed on one damage site by three steps, with exposure time of 0.30, 0.36, and 0.30 ms, and the interval was 1 s. The profile and depth of the CO_2 laser-treated damage site were measured using a profilemeter (Zygo Inc.). The CO_2 laser pulses could create a typically smooth Gaussian-shaped crater with a diameter of about 300 μm by melting or evaporation on fused silica surface. The depth of the mitigated craters was about 2–10 μm, determined mainly by the depth of the damage sites before mitigation.

A Nd:YAG laser was used to determine the damage threshold and damage growth coefficient, which emitted 355-nm, 7-ns, 10-Hz, near-Gaussian beam profile pulses. Laser pulses were focused on the sample surface. The focused laser beam dimensions were 616 and 317 μm on the x and y axes (with an area of 0.153 mm^2), respectively.

The area of damage sites as a function of successive pulse number was measured to determine the damage growth coefficient. The diagnostics to measure the growth included a white-light illuminated, long-working-distance microscope with charge-coupled device (CCD) camera. All samples were oriented with the damage site on the exit surface for the growth measurements. Small initial damage sites initiated by high fluence were chosen to grow under successive pulses of low fluence.

After damage mitigation with CO_2 laser, post-annealing was used to release the residual stresses of CO_2 laser mitigation, with an annealing temperature of 900 °C, holding time of 3 h, and then the samples were cooled to room temperature in the furnace. Acid etching with a buffered HF solution (1% HF+15% NH_4F) for 10 min was also used to remove possible new contaminants during the annealing process. Finally, the damage growth coefficient of the samples with CO_2 laser mitigation followed by annealing treatment was measured.

The threshold fluences of 355-nm laser by R-on-1 damage tests of untreated samples and CO_2 laser mitigated damage sites on fused silica are shown in Fig. 1. In the R-on-1 test, the fluence gradually ramped up to the damaging fluence. Three shots were irradiated at each fluence level. The fluence increased with each increment of about 1.3 J/cm^2 from a starting fluence of about 5.0 J/cm^2. The laser-induced damage thresholds (LIDTs) of 16 CO_2 laser-mitigated damage sites were tested. The effects of mitigation damage and conditioning can be seen with the comparison of the results. As shown in Fig. 1, the LIDT fluence of CO_2 laser mitigated damage sites is higher than that in the untreated samples. The LIDT fluence of CO_2 laser-mitigated damage sites increases and is similar to what has been reported previously[19,20]. Furthermore, the damage threshold of CO_2 laser mitigated damage sites on the exit surface is almost as high as that of the original sample in the entrance surface case. Thus, the damage sometimes occurred on the entrance surface but not on the exit surface during tests, as shown in Fig. 2.

Multi-pulses at some fluence were also used to examine the CO_2 laser mitigation effect. The mitigated sites survived 500 pulses irradiation of 355-nm laser at 13.3 J/cm^2, 65 pulses at 14.7 J/cm^2, 27 pulses at 17.0 J/cm^2, and 1 pulse at 19.3 J/cm^2. After CO_2 treatment, the damage threshold and the multi-pulse irradiation resistance performance under 355-nm laser of the damage sites were obviously increased.

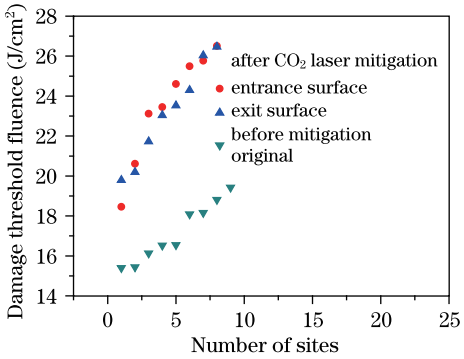

Fig. 1. Damage threshold fluences of 355-nm laser by R-on-1 damage tests of untreated samples and CO_2 laser-mitigated damage sites on fused silica.

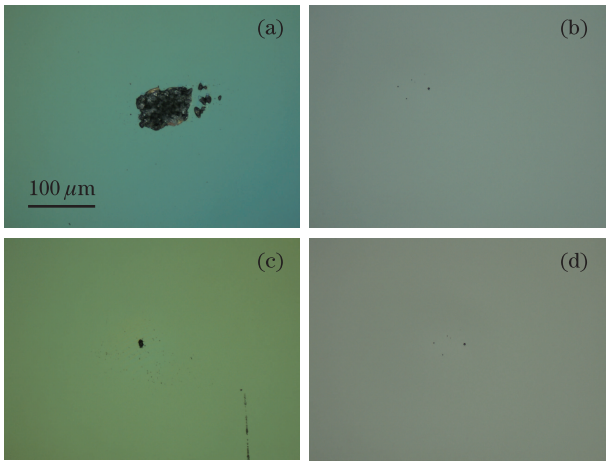

Fig. 2. Optical microscope morphology of damage site A (a) before and (b) after CO_2 laser mitigation; (c) new damage site occurs on the entrance surface and (d) no damage occurs on the exit surface after R-on-1 damage tests by 355-nm laser.

During the damage mitigation testing, as well as the successive testing of LIDT and damage growth coefficient, the CO_2 laser pulses or 355-nm laser pulses were irradiated almost at the center of the damage sites after the fused silica sample was adjusted on a three-dimensional translation stage with a precision of 10 μm. The LIDT results were nearer to the center of the CO_2 laser treated zone. The effect of the whole CO_2 laser treated area, including the laser-affected zone on damage growth, was also considered.

The damage growth measurements consisted of irradiating a damage site at constant fluence and measuring the area of the site after each shot. The 355-nm laser induced damage was often located on the exit surface of fused silica optics. The area of growth followed an exponential dependence to the shot number. A growth curve of a typical site on the exit surface is plotted in Fig. 3. For a small Gaussian beam used, the damage growth progressed in two stages[21]. The transition between the two stages occurred when the damage area reached a damaging beam size (size of the beam where the fluence was above the damage growth threshold). In the first stage, the area of the damage spot increased with the number of pulses in an accelerated manner, as can be very well approximated by an exponential function. The data were fit to an exponential curve given by

$$A = A_0 \mathrm{e}^{\alpha N}, \tag{1}$$

where A is the lateral area of the damage, N is the shot number, and α refers to the growth coefficient. After CO_2 laser treatment, the damage coefficient increased from 0.289 in the original sample to 0.423 at 5.3 J/cm^2.

Growth coefficients versus laser fluence of samples with or without CO_2 laser mitigation and post-heating treatment are shown in Fig. 4. If new damage occurred on the sites with CO_2 laser mitigation, the lateral damage area increased faster than the damage pits on the original sample with the number of shots. For the exit-surface sites, generally speaking the pit was deep with a crater-like appearance and was surrounded by a crack network. The damage growth in fused silica was closely linked to the

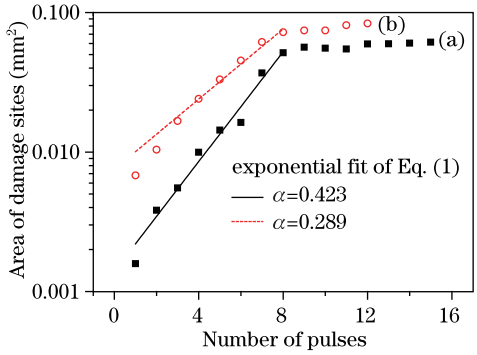

Fig. 3. Area growth behavior of typical damage sites on the exit surface under 355-nm laser irradiation at 5.3 J/cm^2. (a) Site by CO_2 laser mitigation and (b) original sample.

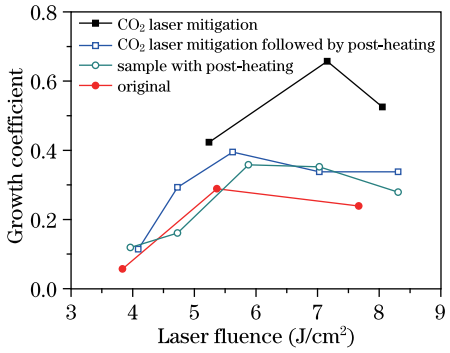

Fig. 4. Growth coefficient versus laser fluence of samples with or without CO_2 laser mitigation and post-heating treatment.

modification of silica during damage initiation[2,22,23]. The high-temperature plasma were associated with initiation or growth phenomena and its associated shock wave in the material created structural and chemical defects in the SiO_2, which could enhance the absorption of subsequent laser pulses. The typical morphology in the form of cracks was represented by a concentric fractured shell. Photoluminescence spectroscopy indicated the formation of absorbing defects within the damage sites[14], including oxygen deficiencies, non-bridging oxygen hole centers, and nonstoichiometric materials. After being treated with CO_2 laser mitigation, the crack became more serious due to the residual stress surrounding the treated sites.

Even after the application of a suitable second laser heating, the residual stress still existed and was prone to damage[16]. Residual stress was the main reason for the increase in damage growth coefficient. Post-heating was used for stress relief. As shown in Fig. 4, the damage growth coefficient of samples with CO_2 laser mitigation followed by post-heating treatment decreases again and becomes almost equal to the original sample.

In conclusion, the initial damage density and damage growth on fused silica versus laser pulsed fluence are measured using a Nd:YAG laser before and after CO_2 laser mitigation. CO_2 laser mitigation followed by post-heating treatment is beneficial to decreasing the damage growth coefficient of samples through CO_2 laser mitigation. Thus, damage mitigation would lead to longer operation lifetime under special fluence application.

References

1. L. Gallais, P. Cormont, and J.-L. Rullier, Opt. Express **17,** 23488 (2009).
2. J. Wong, J. L. Ferriera, E. F. Lindsey, D. L. Haupt, I. D. Hutcheon, and J. H. Kinney, J. Non-Cryst. Solids **352,** 255 (2006).
3. S. Xu, X. Zu, X. Jiang, X. Yuan, J. Huang, H. Wang, H. Lv, and W. Zheng, Nucl. Instrum. Methods Phys. Res. B **266,** 2936 (2008).
4. M. A. Norton, E. E. Donohue, M. D. Feit, R. P. Hackel, W. G. Hollingsworth, A. M. Rubenchik, and M. L. Spaeth, Proc. SPIE **6403,** 64030L (2007).
5. M. A. Norton, L. W. Hrubesh, Z. Wu, E. E. Donohue, M. D. Feit, M. R. Kozlowski, D. Milam, K. P. Neeb, W. A. Molander, A. M. Rubenchik, W. D. Sell, and P. Wegner, LLNL UCRL-JC-139624 (2001).
6. L. W. Hrubesh, M. A. Norton, W. A. Molander, E. E. Donohue, S. M. Maricle, B. M. Penetrante, R. M. Brusasco, W. Grundler, J. A. Butler, J. W. Carr, R. M. Hill, L. J. Summers, M. D. Feit, A. Rubenchik, M. H. Key, P. J. Wegner, A. K. Burnham, L. A. Hackel, and M. R. Kozlowski, Proc. SPIE **4679,** 23 (2002).
7. R. M. Brusasco, B. M. Penetrante, J. A. Butler, and L. W. Hrubesh, Proc. SPIE **4679,** 40 (2002).
8. I. L. Bass, G. M. Guss, and R. P. Hackel, Proc. SPIE **5991,** 59910C (2005).
9. E. Mendez, K. M. Nowak, H. J. Baker, F. J. Villarreal, and D. R. Hall, Appl. Opt. **45,** 5358 (2006).
10. G. Guss, I. Bass, V. Draggoo, R. Hackel, S. Payne, M. J. Lancaster, and P. Mak, Proc. SPIE **6403,** 64030M (2007).
11. S. Palmier, L. Gallais, M. Commandré, P. Cormont, R. Courchinoux, L. Lamaignère, J. L. Rullier, and P. Legros, Appl. Surf. Sci. **255,** 5532 (2009).
12. S. T. Yang, M. J. Matthews, S. Elhadj, D. Cooke, G. M. Guss, V. G. Draggoo, and P. J. Wegner, Appl. Opt. **49,** 2606 (2010).
13. M. J. Matthews, I. L. Bass, G. M. Guss, C. C. Widmayer, and F. L. Ravizza, Proc. SPIE **6720,** 67200A (2007).
14. R. N. Raman, M. J. Matthews, J. J. Adams, and S. G. Demos, Opt. Express **18,** 15207 (2010).
15. M. A. Stevens-Kalceff and J. Wong, J. Appl. Phys. **97,** 113519 (2005).
16. P. Cormont, L. Gallais, L. Lamaignère, J. L. Rullier, P. Combis, and D. Hebert, Opt. Express **18,** 26068 (2010).
17. J. Yoshiyama, F. Y. Génin, A. Salleo, I. Thomas, M. R. Kozlowski, L. M. Sheehan, I. D. Hutcheon, and D. W. Camp, Proc. SPIE **3244,** 331 (1998).
18. B. Ma, Z. Shen, P. He, Y. Ji, T. Sang, H. Liu, D. Liu, and Z. Wang, Chin. Opt. Lett. **8,** 296 (2010).
19. W. Dai, X. Xiang, Y. Jiang, H. J. Wang, X. B. Li, X. D. Yuan, W. G. Zheng, H. B. Lv, and X. T. Zu, Opt. Laser Eng. **49,** 273 (2011).
20. J. Huang, S. Zhao, H. Wang, H. Lü, L. Ye, X. Jiang, X. Yuan, and W. Zheng, Chinese J. Lasers (in Chinese) **36,** 1282 (2009).
21. A. Salleo, R. Chinsio, and F. Y. Génin, Proc. SPIE **3578,** 456 (1999).
22. M. A. Stevens-Kalceff, A. Stesmans, and J. Wong, Appl. Phys. Lett. **80,** 758 (2002).
23. S. Papernov and A. W. Schmid, Proc. SPIE **7132,** 71321J (2008).